

12
5-1-95 JSD

UCRL-ID-119045

Differencing the Diffusion Equation on
Unstructured Meshes in 2-D

Todd S Palmer

October 24, 1994

Lawrence
Livermore
National
Laboratory

This is an informal report intended primarily for internal or limited external distribution. The opinions and conclusions stated are those of the author and may or may not be those of the Laboratory.
Work performed under the auspices of the U.S. Department of Energy by the Lawrence Livermore National Laboratory under Contract W-7405-Eng-48.

DISTRIBUTION OF THIS DOCUMENT IS UNLIMITED

DISCLAIMER

This document was prepared as an account of work sponsored by an agency of the United States Government. Neither the United States Government nor the University of California nor any of their employees, makes any warranty, express or implied, or assumes any legal liability or responsibility for the accuracy, completeness, or usefulness of any information, apparatus, product, or process disclosed, or represents that its use would not infringe privately owned rights. Reference herein to any specific commercial products, process, or service by trade name, trademark, manufacturer, or otherwise, does not necessarily constitute or imply its endorsement, recommendation, or favoring by the United States Government or the University of California. The views and opinions of authors expressed herein do not necessarily state or reflect those of the United States Government or the University of California, and shall not be used for advertising or product endorsement purposes.

This report has been reproduced
directly from the best available copy.

Available to DOE and DOE contractors from the
Office of Scientific and Technical Information
P.O. Box 62, Oak Ridge, TN 37831
Prices available from (615) 576-8401, FTS 626-8401

Available to the public from the
National Technical Information Service
U.S. Department of Commerce
5285 Port Royal Rd.,
Springfield, VA 22161

Differencing the Diffusion Equation on Unstructured Meshes in 2-D

Todd S. Palmer
Lawrence Livermore National Laboratory
Livermore, California 94550

INTRODUCTION

During the last few years, there has been an increased effort to devise robust transport differencings for unstructured meshes, specifically arbitrarily connected grids of *polygons*. Adams^{1,2,3} has investigated unstructured mesh discretization techniques for the even- and odd-parity forms of the transport equation, and for the more traditional first-order form. Conversely, development of unstructured mesh diffusion methods has been lacking. While Morel⁴, Kershaw⁵, Shestakov⁶ and others have done a great deal of work on diffusion schemes for logically-rectangular grids, to our knowledge there has been no work on discretizations of the diffusion equation on unstructured meshes of polygons.

In this paper, we introduce a point-centered diffusion differencing for two-dimensional unstructured meshes. We have designed the method to have the following attractive properties: 1) the scheme is equivalent to the standard five-point point-centered scheme on an orthogonal mesh; 2) the method preserves the homogeneous linear solution; 3) the method gives second-order accuracy; 4) we have strict conservation within the control volume surrounding each point; and 5) the numerical solution converges to the exact result as the mesh is refined, regardless of the smoothness of the mesh. A potential disadvantage of the method is that the diffusion matrix is *asymmetric*, in general.

DERIVATION OF THE METHOD

We begin with the time-independent one-group diffusion equation, written as two first order equations,

$$\nabla \cdot J + \sigma_a \phi = Q, \quad (1)$$

$$J = -D \nabla \phi \quad (2)$$

We now consider an unstructured mesh in $r - z$ geometry, as shown in Figure 1. Each polygonal cell is divided into subcell volumes called *corners*. In two dimensions the corner is a quadrilateral formed by connecting the zone-center with the midpoint of each edge surrounding the zone. Figure 2 illustrates a corner in a typical polygonal zone. Our goal is to formulate a discretized diffusion equation in terms of point-centered differences.

Our first step is to enforce particle balance by integrating Eq. (1) over the control volume associated with the point of interest. This control volume is defined to be the union of all

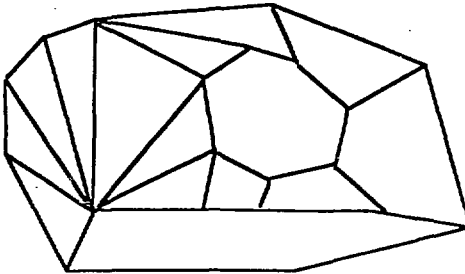


Figure 1: A Portion of an Unstructured Mesh.

corners surrounding the specified point. After performing this integration, we obtain

$$\sum_{c \in p} A_{c+1/2} \cdot J_{c+1/2} + A_{c-1/2} \cdot J_{c-1/2} + \left(\sum_{c \in p} V_c \sigma_{a,c} \right) \phi_p = \sum_{c \in p} V_c Q_c. \quad (3)$$

Referring again to Figure 2, V_c is the volume of corner c , $A_{c+1/2}$ and $A_{c-1/2}$ are the areas of the edges $c+1/2$ and $c-1/2$ multiplied by their respective unit outward normal vectors, ϕ_p is the average flux in the control volume associated with point p , and the notation $c \in p$ refers to all the corners c which surround the point p .

The next step in our derivation is the elimination of the edge currents $J_{c+1/2}$ and $J_{c-1/2}$. We do this by defining them in terms of point-centered fluxes ϕ_p and fluxes at the zone-centers ϕ_z . Focusing now on the first term in Eq. (3), we can write

$$\begin{aligned} A_{c+1/2} \cdot J_{c+1/2} &= -D_c A_{c+1/2} (\vec{n} \cdot \vec{\nabla} \phi) \Big|_p \\ &= -D_c A_{c+1/2} (\vec{n} \cdot \vec{\nabla} \phi) \Big|_{z+1/2}. \end{aligned} \quad (4)$$

Referring to Figure 3, we can use Eq. (2) to replace the gradient terms in Eq. (4) with

$$\frac{1}{2} (\vec{n} \cdot \vec{\nabla} \phi) \Big|_{z+1/2} = \frac{\phi_{z+1} - \phi_z}{s_{c+1} \sin \theta_c}, \quad (5)$$

$$\frac{1}{2} (\vec{n} \cdot \vec{\nabla} \phi) \Big|_{z-1/2} = \frac{\phi_z - \phi_{z-1}}{s_{c-1} \sin \theta_c}, \quad (6)$$

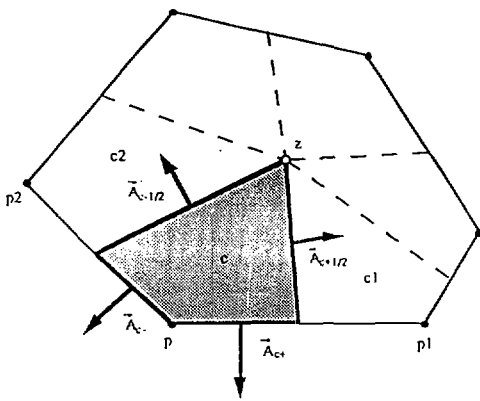


Figure 2: A Corner and its Bounding Surfaces.

Simple linear interpolations and extrapolations allow us to write,

$$\phi_4 = \left(\frac{s_{c4+1/2} \cdot s_{c4}}{s_{c4+1/2}^2} \right) \phi_1 + \left(1 + \frac{s_{c4+1/2} \cdot s_{c4}}{s_{c4+1/2}^2} \right) \phi_{4+}, \quad (7)$$

$$\phi_4 = \left(\frac{s_{c4+1/2} \cdot s_{c4}}{s_{c4+1/2}^2} \right) \phi_1 + \left(1 - \frac{s_{c4+1/2} \cdot s_{c4}}{s_{c4+1/2}^2} \right) \phi_{4-}, \quad (8)$$

If we substitute Eqs. (7) and (8) into Eqs. (5) and (6), we find that we can obtain a formula for ϕ_4 of the form

$$\phi_4 = \frac{D_{c4} \phi_{p1} + D_c \phi_p + \left(\frac{s_{c4+1/2} \cdot s_{c4}}{s_{c4+1/2}^2} \right) \phi_2}{D_{c1} + D_c + \left(\frac{s_{c4+1/2} \cdot s_{c4}}{s_{c4+1/2}^2} \right)}. \quad (9)$$

Using our expression for ϕ_{c4} , we can now write $A_{c4+1/2} \cdot J_{c4+1/2}$ as

$$A_{c4+1/2} \cdot J_{c4+1/2} = \left\{ D_c \lambda_{c4+1/2} \left[\left(\frac{1}{s_{c4+1/2} \cdot s_{c4}} \right) \phi_p + \left(\frac{\cot \theta_c}{s_{c4+1/2}} \right) \phi_c \right. \right. \\ \left. \left. + \left(\frac{1}{s_{c4+1/2} \cdot s_1 \theta_c} - \frac{\cot \theta_c}{s_{c4+1/2}} \right) [x_1 \phi_{p1} + x_2 \phi_2 + \phi_4] - (x_1 - x_2) \phi_4 \right] \right\}. \quad (10)$$

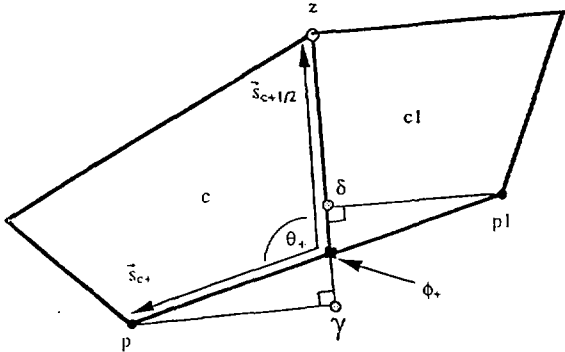


Figure 3: The gradient calculation for $\overline{A_{c+1/2}} \cdot \overline{J_{c+1/2}}$.

where we have defined x_1 and x_2 to be

$$x_1 = \frac{D_{e1}}{D_{e1} + D_e + (D_e - D_{e1}) \left(\frac{S_{e1} + \sqrt{2} \frac{S_e}{\sum_{i \in \mathcal{E}} S_i}}{2} \right)}, \quad (11)$$

$$x_2 := \frac{D_e}{D_{ee} + D_e + (D_e - D_{ee}) \left(\frac{S_{e+1}/2 - S_{e+1}}{\sum_i P_i} \right)} \quad (12)$$

We can now go through the same steps to obtain a formula for $A_{e-1/2}^{+1/2} \cdot J_{e-1/2}^{+1/2}$. The final result, referring to Figure 4 is

$$\begin{aligned}
& \left. \left(\frac{1}{S_{i-1/2}} \partial_{\theta} J_{i-1/2}^{\pm} - D_i A_{i-1/2} \right) \left(\begin{array}{c} 1 \\ \sin \theta \end{array} \right) \phi_p + \left(\begin{array}{c} \cot \theta \\ S_{i-1/2} \end{array} \right) \phi_s \right. \\
& \left. + \left(\begin{array}{cc} 1 & \cot \theta \\ \sin \theta & S_{i-1} \end{array} \right) (p_i \psi_p^{\pm} + p_i x \phi_p^{\pm} + t) - (p_i - q_i) \phi_s \right\}, \quad (13)
\end{aligned}$$

where we have defined q_1 and q_2 to be

$$q^* = \min_{\{i_1, i_2, i_3\} \subseteq \{1, 2, \dots, n\}} \Omega_{i_1 i_2 i_3} \left(S_{i_1} \left(\frac{S_{i_2}}{S_{i_1}}, \frac{S_{i_3}}{S_{i_1}} \right) \right) \quad (14)$$

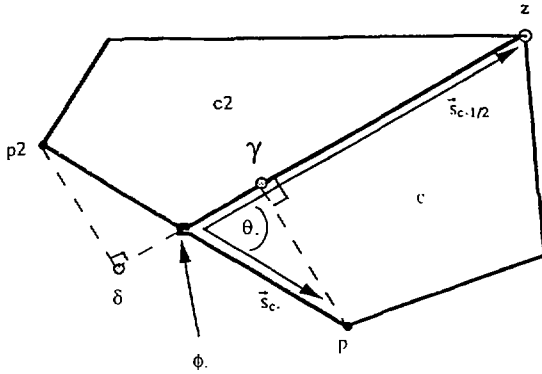


Figure 4: The gradient calculation for $A_{c-1/2} \cdot \vec{s}_{c-1/2}$.

$$y_2 = \frac{D_{c2}}{D_{c2} + D_c + (D_c - D_{c2}) \left(\frac{s_{c-1/2}}{s_c} \right)}, \quad (15)$$

At this point, our diffusion equation is written in terms of the point fluxes ϕ_p and the zone-center fluxes ϕ_c . Our last task is to define these zone-center fluxes as functions of the point fluxes. We do this by first defining a zone-averaged gradient $\langle \nabla \phi \rangle_z$,

$$\begin{aligned} \langle \nabla \phi \rangle_z &= \frac{1}{A_z} \int d^2 r \langle \nabla \phi \rangle, \\ &= \frac{1}{A_z} \int ds \vec{n} \phi, \end{aligned} \quad (16)$$

where A_z is the area of the zone, and \vec{n} is the unit outward normal to the surface of the zone. In general, the zone-averaged gradient is a function of the fluxes at all the points surrounding the zone. This average gradient can now be used to define the zone-center flux. We define this flux to be a weighted average of extrapolations from the point fluxes surrounding the zone, i.e.

$$\phi_c = \frac{\sum_{p \in \partial z} w_p \left(\phi_p + \frac{s^2}{s_{p-z}} (\phi_{p+1/2} - \phi_{p-1/2}) \right)}{\sum_p w_p} \quad (17)$$

We define the weights w_p to be inverse length weights,

$$w_p = \frac{1}{s_{p \rightarrow z}}, \quad (18)$$

where $s_{p \rightarrow z}$ is the distance from the point p to the zone-center z . This allows us to eliminate the cell center flux in terms of the point fluxes. Morel's⁴ cell-center method, which has many of the same attractive characteristics as our method, is forced to retain two kinds of unknowns (cell-center and cell-edge fluxes), while we have only one kind (point fluxes).

This completely defines our unstructured diffusion method, aside from boundary conditions. In general, each point is connected to every point associated with the zones surrounding that point. On an orthogonal mesh, the connectivity reduces to the standard point-centered five-point stencil.

NUMERICAL RESULTS

In this section, we present the results of a few test problems designed to demonstrate that our method preserves the linear solution and is second-order accurate. First we consider the following test problem in a unit cylinder,

$$-\frac{\partial}{\partial z} D \frac{\partial \phi}{\partial z} = 0, \quad (19)$$

$$\phi(r, 1 + 2D) = 1, \quad (20)$$

$$J_{\text{ext}}(r, 0) - \frac{1}{4} \phi(r, 0) + \frac{D}{2} \frac{\partial \phi}{\partial z}(r, 0) \neq 0, \quad (21)$$

$$J(0, z) = \overline{J}(1, z) = 0, \quad (22)$$

where we have chosen D to be 1.0. We solve this problem on four different meshes: 1) Kershaw's "z-mesh" as seen in Figure 5; 2) the all-triangle mesh shown in Figure 6, 3) Shestakov's random mesh, shown in Figure 7, and (4) Shestakov's parabolic mesh, shown in Figure 8. The exact solution to this problem is linear in the z coordinate,

$$\phi(r, z) = \frac{z + 2D}{1 + 4D}. \quad (23)$$

Figure 9 is a contour plot of the solution of this problem on Kershaw's "z-mesh". Notice that the contours are exactly linear. In fact, we obtain the exact solution for this problem, independent of the mesh we are using. This is an important result because other diffusion methods have trouble obtaining the linear solution on these meshes. Specifically, Kershaw's finite difference method will not produce a linear solution on the "z-mesh," the random problem's "z-mesh" is not linear, and the diffusion coefficient is slightly linear on the "z-mesh," but on the random mesh a parallelogram flux perturb the solution, slightly away from linearity.

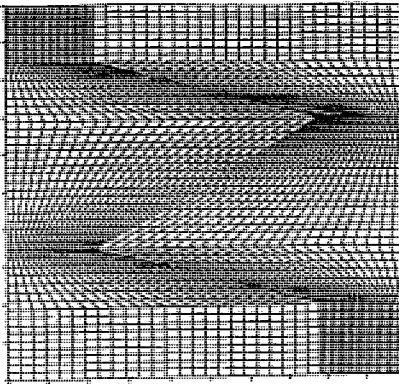


Figure 5: Kershaw's "z-mesh".

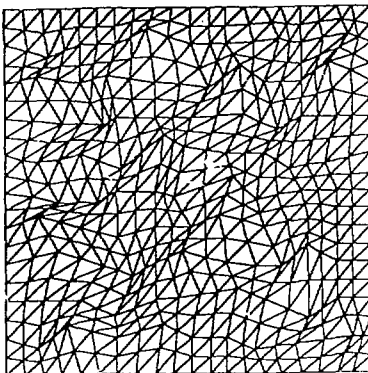


Figure 6: An all triangle mesh.

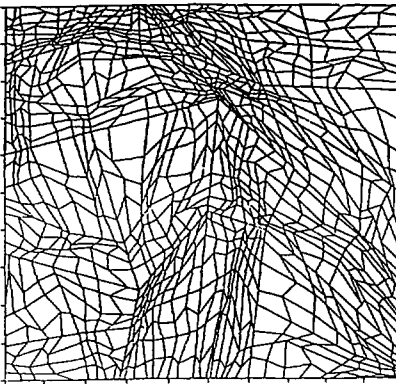


Figure 7: Shestakov's random mesh.

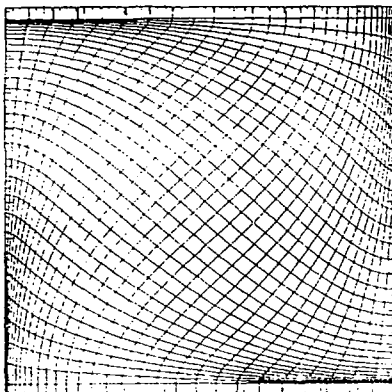


Figure 8: Shestakov's parabolic mesh.

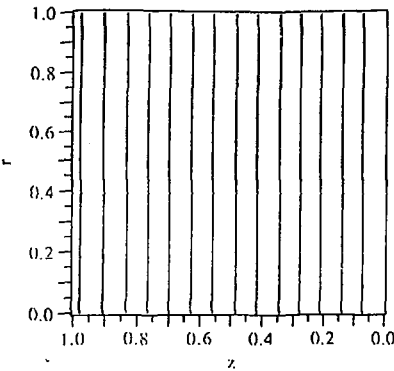


Figure 9: Contours of the solution to Kershaw's "z-mesh" problem.

A second test problem, designed to illustrate that this method is second-order accurate, involves the solution of the following diffusion problem:

$$\frac{\partial}{\partial r} D \frac{\partial \phi}{\partial z} = z^2, \quad (24)$$

$$\phi(r, 1 + 2D) = 1, \quad (25)$$

$$\phi(r = 2D) = 0, \quad (26)$$

$$\bar{J}(0, z) = \bar{J}(1, z) = 0, \quad (27)$$

where we have chosen D to be $\frac{1}{30}$. The exact solution to this problem is quartic in the z coordinate,

$$\phi(r, z) = \frac{1}{12D} \left[\left(\frac{1+8D}{1+4D} \right) (z + 2D) - z^4 \right]. \quad (28)$$

We solve this problem on three different orthogonal and random meshes (20×20 , 40×40 , and 80×80) and observe the change in the L_2 norm of the error as a function of mesh size. A typical random mesh is shown in Figure 10 and Figure 11 is a plot of the error as a function of the mesh size. The results for the 17×17 point centered method are excellent both on the orthogonal and random meshes; the method is indeed second-order accurate. Figure 11 also contains results for the cell center discretization schemes by Morel and Kershaw. It is obvious that Morel's scheme is also second-order accurate, while Kershaw's is not. In fact, Kershaw's scheme does not converge to the analytic solution as the mesh is refined. The other methods, as well as Morel's scheme, converge to the analytic solution.

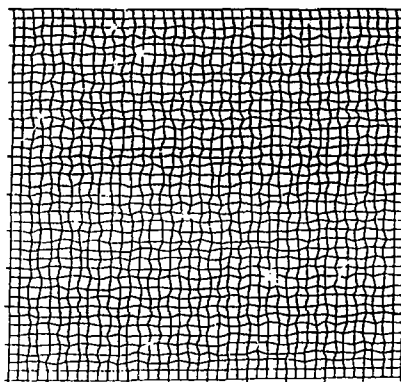


Figure 10: A 40×40 random mesh.

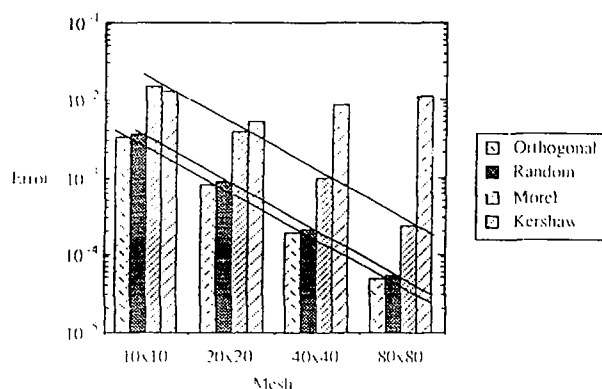


Figure 11: Comparison of error versus mesh size.

CONCLUSIONS

We have been successful in deriving and implementing a diffusion discretization for unstructured meshes in 2-D which has many attractive properties. However there are two issues which must be considered and quantified: 1) the overhead involved in calculating the matrix on an unstructured mesh, and 2) the expense in the iterative solution of the asymmetric matrix. There is no question that navigating on an unstructured mesh *costs* more than on an orthogonal mesh (either in storage or CPU time). Also, depending on the structure of our diffusion matrix, its solution can take significantly longer to obtain. These concerns are being addressed, but are not resolved at this time.

ACKNOWLEDGMENTS

The author would like to thank Marvin Adams and Donald Burton for their comments and suggestions.

REFERENCES

1. M.L. Adams, "A New Transport Discretization Scheme for Arbitrary Spatial Meshes in XY Geometry," Proc. ANS Topical Meeting, Advances in Mathematics, Computations, and Reactor Physics, April 29-May 2, 1991, Pittsburgh, PA, Vol. 3, Sec. 13.2, pp 2-1 through 2-9 (1991).
2. T.S. Palmer, "Curvilinear Geometry Transport Discretizations in Thick, Diffusive Regions", Dissertation, Dept. of Nuclear Engineering, University of Michigan, May, 1993.
3. M.L. Adams, "Discontinuous Finite-Element Transport Solutions in the Thick Diffusion Limit in Cartesian Geometry," Proc. ANS Topical Meeting, Advances in Mathematics, Computations, and Reactor Physics, April 29-May 2, 1991, Pittsburgh, PA, Vol. 5, Sec. 21.1, pp 3-1 through 3-15 (1991).
4. J.E. Morel, J.E. Dendy, Jr., Michael L. Hall and Stephen W. White, "A Cell-Centered Lagrangian-Mesh Diffusion Differencing Scheme," *J. Comp. Phys.*, **103**, 286 (1992).
5. D.S. Kershaw, "Differencing of the Diffusion Equation in Lagrangian Hydrodynamic Codes," *J. Comp. Phys.*, **39**, 375 (1981).
6. A.I. Sheshatov, J.A. Harte, and D.S. Kershaw, "Solution of the Diffusion Equation by Finite Elements in Lagrangian Hydrodynamic Codes," *J. Comp. Phys.*, **76**, 385 (1988).
7. D.E. Burton, "Conservation of Energy, Momentum, and Angular Momentum in Lagrangian Staggered-Grid Hydrodynamics," Lawrence Livermore National Laboratory Report UCRL-JC-105926 (1990).